Account/Revue

Carbohydrate-based fluorometric and colorimetric sensors for Cu^{2+} ion recognition

Samiul Islam Hazarika, Ananta Kumar Atta[*]

Department of Basic & Applied Science, National Institute of Technology Arunachal Pradesh, Yupia, 791112, India

A B S T R A C T

The development of optical sensors using carbohydrates for selective detection of copper in water and living system has been an active research area in the past few years because of widespread applications and biological importance of copper. Introduction of carbohydrate to design the sensors is an attractive field of research because of its chiral entities with hydroxyl groups and oxygen atoms, controlled ring-flipping capability, abundance, and biocompatibility. This minireview focuses on the reported carbohydrate-based fluorescent and colorimetric sensors for Cu^{2+} detection and is organized according to their structural categories such as triazole-linked, imine-linked, and non—triazole-/imine-linked carbohydrate—based sensors. To the best of our knowledge, this is the first review article focused on carbohydrate-based Cu^{2+} sensors.

1. Introduction

Out of various heavy metals, copper is the third-most abundant metal found in the human body and plays an important role in the physiological process [1—3]. Low concentration of Cu^{2+} is required for the living system for growth and development. It also acts as a catalytic cofactor for different types of metalloenzymes [4—6]. In spite of its biological applications, copper is also widely used in domestic purposes and industries because of its high thermal/electrical conductivity, stability, and alloy formation ability with other metals [7—9]. In spite of its importance, high-dose copper can exhibit toxicity and severe neurodegenerative diseases such as prion disease, Alzheimer disease, hypoglycemia, dyslexia, Wilson disease, etc., through the formation of reactive oxygen species (ROS) [10—14]. Moreover, copper acts as a remarkable environmental pollutant because of its use in industrial, household, and agricultural processes [15,16]. Accordingly, the World

Health Organization (WHO) has suggested that the acceptable concentration of copper should be of 31.5 μM in the drinking water [17]. Owing to the Janus-faced properties of copper in the living system, a fast, convenient, cheap, and reliable method for detection Cu^{2+} ions in drinking water and biological systems is important and challenging. In this regard, optical detections (via colorimetric or fluorescence changes) among the other detection techniques are more convenient because of their simplicity, high sensitivity, and finally ability of 'naked-eye' detection of cations or anions [18]. For these reasons, several non-—carbohydrate-based colorimetric or fluorometric sensors have been reported for Cu^{2+} detection [19—28], but most of them suffer from the following disadvantages: poor water solubility, expensive starting materials, longer response time, interference by other cations or anions, and finally toxicity for the cell. In this context, colorimetric and fluorometric sensors based on biologically benign carbohydrates would be more advantageous for the presence of —OH groups, and oxygen atoms in the sugar moiety are very suitable for cation binding and for increasing the water solubility [29—31]. Generally, the carbohydrate-based fluorometric or colorimetric sensors have been

* Corresponding author.
 E-mail addresses: akatta.chem@nitap.ac.in, attaananta@gmail.com (A.K. Atta).

designed with the incorporation of a fluorophore or chromophore. Various forms of carbohydrates, such as open chain, pyranose, and furanose, were used for copper ion detection. The pyranose form of sugar is considered a more suitable ring system to accommodate axial substituents than cyclohexane because anomeric effects of sugar favor the axial orientation of an electronegative substituent at the anomeric position. In spite of that, the axial lone pair of the ring oxygen is less open to 1, 3-diaxial repulsions than the axial hydrogen atom of cyclohexanes [32,33]. This unique phenomenon found in carbohydrates is useful in the detection of ions selectively.

To date, no review articles addressing carbohydrate-based fluorescent and colorimetric sensors for Cu^{2+} ions have been reported. The main purpose of this review is to fill in the gap between carbohydrate-based and non-–carbohydrate-based Cu^{2+} sensors. In the present review, we have tried to summarize all the articles published to date for colorimetric/fluorimetric detection of Cu^{2+} ions by carbohydrate-based (monosaccharide) sensors.

2. Carbohydrate-based triazole-linked sensors

The sensing and complexing capability of 1,2,3-triazole moiety toward cations and anions is remarkable [34]. In addition, the use of the triazole group as a linker has been applied in various fields, including drug design, bioconjugation, and materials chemistry [35,36]. In view of this, Hseih et al. [37] reported bis-triazolyl sugar-aza-crown (SAC) ether fluorescent sensor **1** (Fig. 1) for selective detection of Cu^{2+} and Hg^{2+}, where triazole groups provide suitable binding sites and anthracene moieties act as the signaling units. Two anthracenetriazolymethyl molecules containing sensor **1** exhibited dual signaling behaviors for Cu^{2+} and Hg^{2+} in methanol. Fluorescent intensity of **1** was examined in different solvents, namely, methanol, dichloromethane, and acetonitrile. Sensor **1** exhibited the highest emission in methanol solvent. The fluorescence of **1** was quenched by Cu^{2+}, Hg^{2+}, Ni^{2+}, and Co^{2+} ions over the several metal ions. But, more effectively, fluorescence was

quenched by Cu^{2+} and Hg^{2+} ions because of reverse photoinduced electron transfer (PET) from the excited anthracene units to triazole moieties [38–40]. The fluorescence intensity of **1** was quenched effectively 82% for Hg^{2+} and 92% for Cu^{2+}. From the fluorescence titration experiment, the binding constant (Ka) and the detection limit of **1** for Cu^{2+} were calculated and found to be 4×10^5 M^{-1} and 1.39×10^{-6} M, respectively. The 1:1 stoichiometry of the **1**·Cu^{2+} complex was obtained from a Job plot. To establish the binding mode of **1** with Cu^{2+} ions, ^{1}H NMR titration was carried out in the presence of Hg^{2+} ion because of the paramagnetic nature of copper. From the ^{1}H NMR titration experiment, they concluded that a significant conformational change of the SAC ring occurred after copper complex formation.

The same group has reported another SAC ether–based cavitand **2** (Fig. 2) for selective recognition of Cu^{2+} in methanol [41]. In the presence of the Cu^{2+} ions, the fluorescence intensity of **2** was enhanced via the PET process upon complexation of the nitrogen atoms by the metal ion. These results indicate that Cu^{2+} is recognized by either the triazole moieties or two linker nitrogen atoms of the sensor **2**. The fluorescence quenching was observed after addition of 10 equiv of Hg^{2+} to the solution of the **2**·Cu^{2+} complex, which was explained by the presence of two different recognition sites in SAC ether **2**. The actual binding mechanism for both ions is not reported in the article. Fluorescence titration indicates that the fluorescence intensity of **2** increased with increasing concentration of Cu^{2+} ions. In addition to the Cu^{2+}-sensing property of **2**, the recognition ability of **2** with anions was also investigated. This experiment indicated that the fluorescence intensity of **2** was not affected in the presence of anions such as F$^-$, Cl$^-$, Br$^-$, and I$^-$. The association constant (K_a) of **2** for Cu^{2+} was found to be 2.5×10^4 M^{-1} from the Stern–Volmer plot, and the detection limit was estimated to be 1.39×10^{-6} M in MeOH from fluorescence titration. The Job plot indicated the formation of the 1:1 complex between **2** and Cu^{2+} ions.
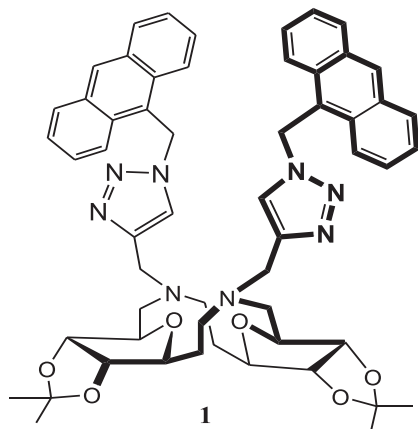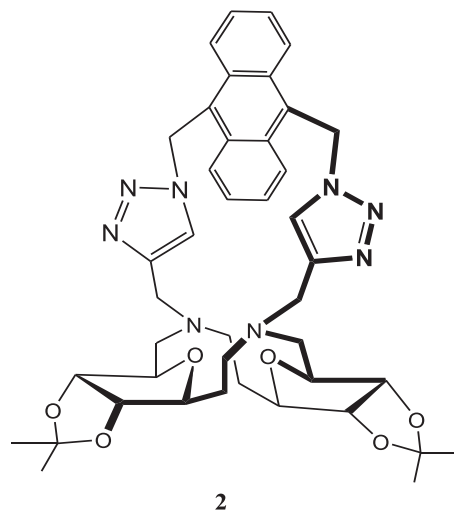

Fig. 1. Sugar-aza-crown (SAC) ether **1**.

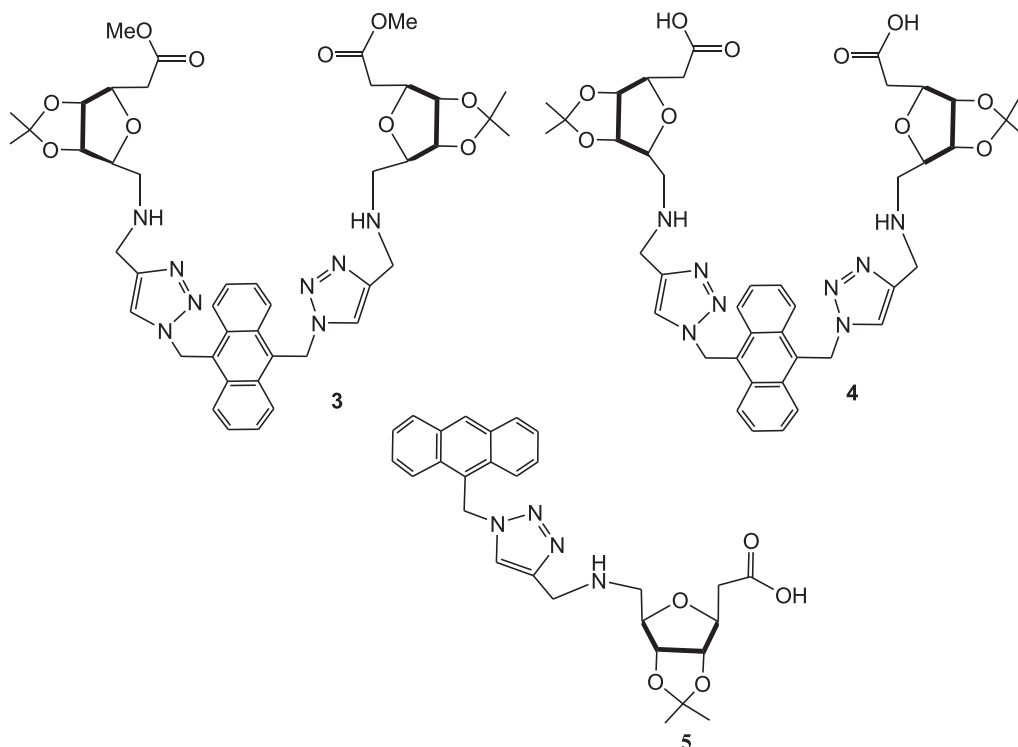**Fig. 2.** Sugar-aza-crown (SAC) ether–based cavitand **2**.

Fig. 3. Ribosyl-based triazolyl fluorescent sensors **3, 4,** and reference compound **5**.

The triazole-linked ribosyl-based ester ending "on-off" fluorescence sensor **3** (Fig. 3) exhibits selectivity toward Cu²⁺ and Ni²⁺ in methanol [42]. To increase the water solubility, the ester end groups of **3** have been hydrolyzed and completely water-soluble fluorescent sensor **4** has been synthesized (Fig. 3), which showed high selectivity toward Cu²⁺ and Hg²⁺ ions in water medium [43], whereas the control compound **5** (Fig. 3) exhibited poor selectivity toward metal ions. Huang et al. [42] claimed that the ribosyl functionalities of sensor **4** act as a scaffold to bring
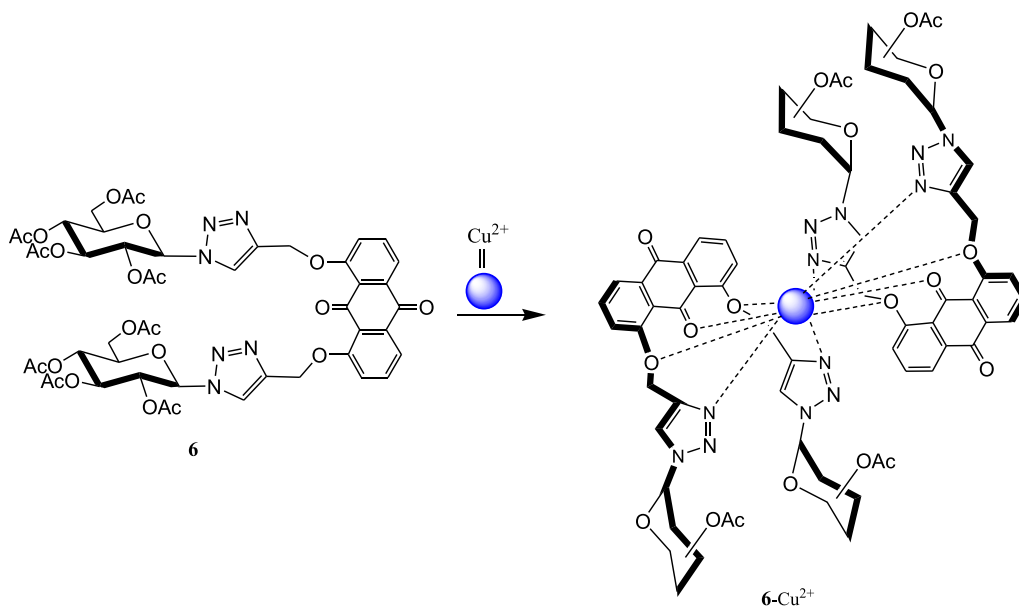

Fig. 4. Triazole-linked glucosyl anthraquinone **6** and possible binding mode of the **6**·Cu²⁺ complex.
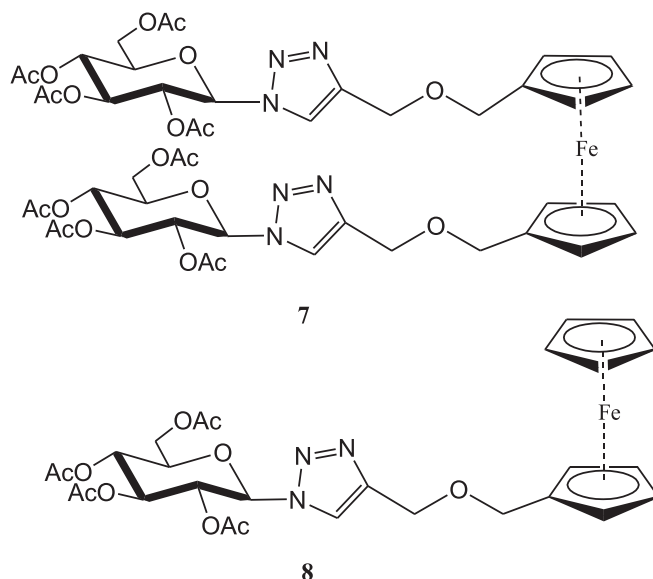
Fig. 5. Triazole-linked monoferrocene-carbohydrate and diferrocene-carbohydrate conjugates **7** and **8**.

two triazole groups on the same side and enhanced the quenching effect in the presence of Cu^{2+} or Hg^{2+}. The association constant (K_a) of $4 \cdot Cu^{2+}$ was calculated as $2.15 \times 10^5\ M^{-1}$ from fluorescence titration spectroscopy. In the Job plot, maximum fluorescence emission was noticed when the mole fraction of Cu^{2+} was 0.5, which suggested the formation of a 1:1 metal–ligand complex. The limit of detection of **4** for the analyte Cu^{2+} was calculated as 0.89 μM.

Zhang et al. [44] reported a triazole-linked glucosyl anthraquinone **6** (Fig. 4) for selective detection of Cu^{2+} ions. The photophysical properties of **6** were scrutinized with absorbance and fluorescence studies in the presence of several metal ions. In the absorption spectra, remarkable blue shift ($\Delta\lambda = 70$ nm) and intensity enhancement were noticed after addition of Cu^{2+} in the sensor solution, whereas the fluorescence of **6** quenched effectively in the presence of Cu^{2+} under the same experimental condition. The Job plot experiment of the $6 \cdot Cu^{2+}$ complex was carried out by fluorescence spectroscopy, which exhibited a metal-ligand binding ratio of 1:2. The association constant (log K_a) of the $6 \cdot Cu^{2+}$ complex was obtained from fluorescence titration spectrometry and found to be 5.64. The optical selectivity of **6** toward Cu^{2+} was explained through intramolecular charge transfer (ICT) [45] and anthraquinone $\rightarrow$ Cu^{2+} μ-cation interaction [46] and/or paramagnetic nature of Cu^{2+} [47,48]. ^{1}H NMR spectra of **6** in the presence of various concentrations of Cu^{2+} suggested that the triazole moiety and ether oxygen of anthraquinone directly participated in the binding event (Fig. 4).

Triazole-based ferrocene-carbohydrate bioconjugates **7** and **8** (Fig. 5) have been developed by Thakur et al. [49] for selective recognition of Cu^{2+} in CH_3CN/H_2O (1:4, v/v). The complexation properties of **7** and **8** with Cu^{2+} ions in CH_3CN have been confirmed by electrochemistry and UV-vis spectroscopic measurements. After incremental addition of Cu^{2+} (0–1 equiv) to both sensor solutions, a new and a weak low-energy absorption band at $\lambda = 630$ nm appeared for both cases. This spectral shift explained the color change from yellow to dark green. The color change from yellow to dark green occurred by oxidation of the ferrocene moiety upon complexation with Cu^{2+} ions [50]. The 1:1 stoichiometries of the copper complexes were established from Job plot experiments using UV-vis titration data. The metal–ligand binding ratio (1:1) was further supported by the high-resolution mass spectra (HRMS) experiment of the complex.
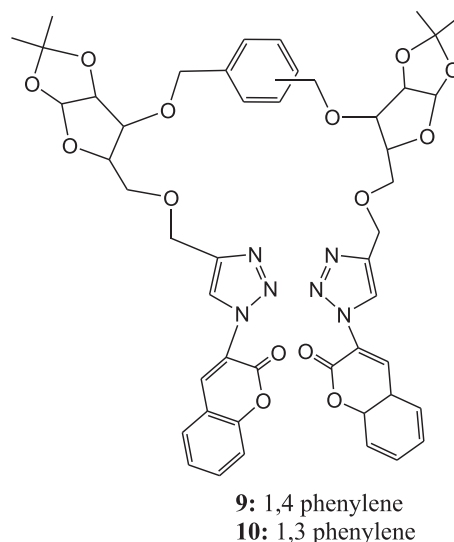

9: 1,4 phenylene
10: 1,3 phenylene

Fig. 6. Bis-triazolyl-linked glycosyl fluorescent sensors **9** and **10**.
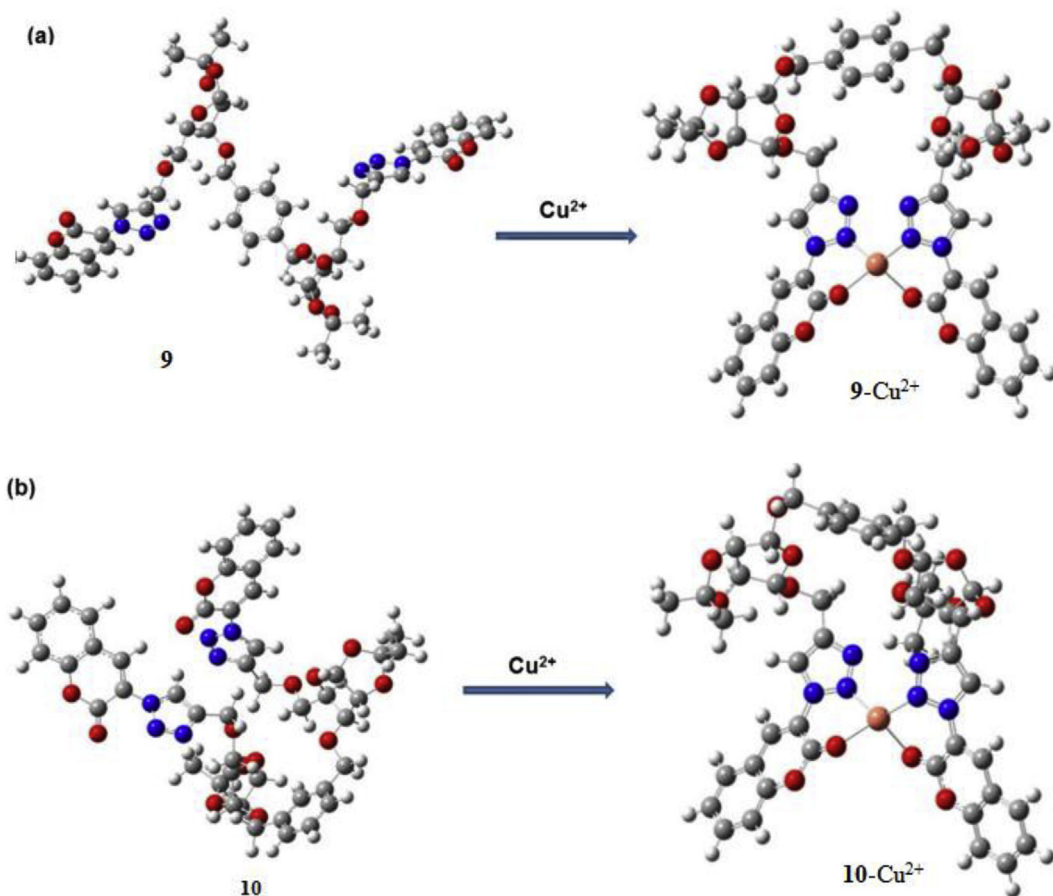
Fig. 7. DFT-optimized structures of (a) **9** and **9**·Cu²⁺; (b) **10** and **10**·Cu²⁺ complexes. DFT, density functional theory.

Kushwaha et al. [51] developed the bis-triazolyl-linked glycosyl fluorescent sensors **9** and **10** (Fig. 6) from 1,2:5,6-di-*O*-isopropylidene-α-ᴅ-glucofuranose for selective detection of Cu²⁺ ions. The fluorescence intensity of **9** and **10** was reduced significantly in the presence of Cu²⁺ ions in acetonitrile solvent. The fluorescence quenching efficiencies $[(I_0-I)/I_0]\times 100$ of **9** and **10** were found to be 70% and 68%, respectively, after addition of 10 equiv of Cu²⁺ ions. The Cu²⁺-induced fluorescence quenching was explained by PET from coumarin to bound Cu²⁺ [52,53].

The formation of the 1:1 complex was confirmed in both cases by Job plot experiments. Furthermore, the binding constants for the complexes (**9**·Cu²⁺ and **10**·Cu²⁺) were calculated from fluorescence titration data using the Benesi-Hildebrand plot and estimated to be 3.34×10^3 M⁻¹ for **9**·Cu²⁺ and 5.93×10^3 M⁻¹ for **10**·Cu²⁺. The detection limits of the sensors **9** and **10** for Cu²⁺ were calculated to be 6.99 μM and 7.30 μM, respectively, from emission titration experiments. The binding mode of each sensor with Cu²⁺ was established from density functional theory (DFT) calculations. The theoretical observation suggested that the optimized structure of sensor **9** exhibited *trans*-configuration and **10** existed *cis*-configuration of triazolocoumarin arms with respect to phenylene ring (Fig. 6). The optimized structures of both complexes (**9**·Cu²⁺ and **10**·Cu²⁺)
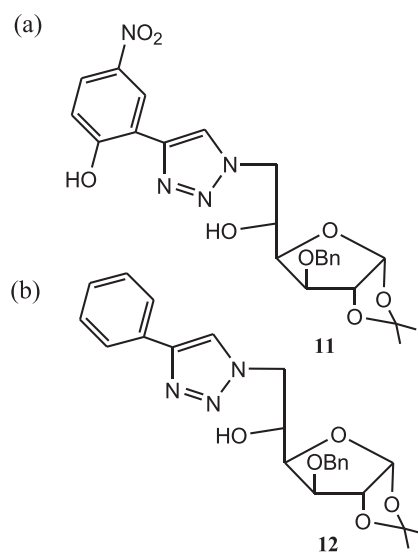

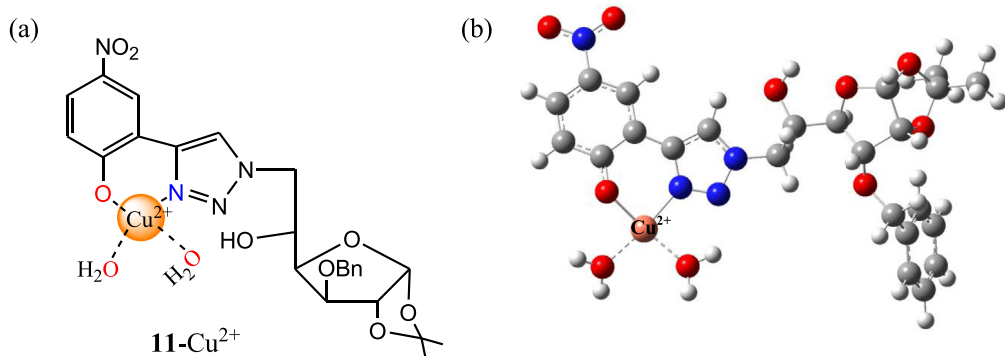Fig. 8. Structures of glucofuranose colorimetric sensor **11** and (b) model compound **12**.

Fig. 9. (a) Proposed binding mode of **11** with Cu^{2+}; (b) DFT-optimized structure of the **11**·Cu^{2+} complex. DFT, density functional theory.

suggested that *N*2 of triazole and oxygen of coumarin carbonyl take part in the binding mechanism (Fig. 7).

Recently, we [54] reported a new and simple triazole-linked glucofuranose derivative **11** (Fig. 8a) for selective colorimetric detection of Cu^{2+} ions in an aqueous medium (CH$_3$CN/phosphate buffer; 1/4, v/v, pH 7.4). The UV-vis absorption and color were remarkably changed in the presence of Cu^{2+} ions over various cations and anions. The binding mode of **11** with Cu^{2+} was established by the synthesized model compound **12** (Fig. 8b). The absorption of **12** was unaffected toward cations and anions, suggesting the involvement of aromatic −OH in the binding mechanism. Sensor **11** exhibited the naked-eye color change from yellow to colorless in the presence of Cu^{2+} ions, which was attributed by the hypsochromic shift of 46 nm of **11** [55]. The metal−ligand binding ratio (1:1) was established from the Job plot using absorption titration data. The 1:1 stoichiometry of the **11**·Cu^{2+} complex was further supported by electrospray ionization mass spectrometry (ESI-MS) spectrometry of the complex.

In addition, the reversible binding mode of **11** with Cu^{2+} was established by ethylenediaminetetraacetic acid (EDTA) experiment. The limit of detection and binding constant of **11** for Cu^{2+} ions were found to be 3.50 μM and 4.2 × 10^5 M^{-1}, respectively. Finally, the binding mode was supported by fourier-transform infrared spectroscopy (FTIR), DFT, and time-dependent density functional theory (TDDFT) calculations and concluded that triazole moiety and aromatic hydroxyl group of **11** are coordinated with Cu^{2+} ions after deprotonation of aromatic −OH group (Fig. 9a). The DFT-optimized structure of the **11**·Cu^{2+} complex is shown in Fig. 9b.
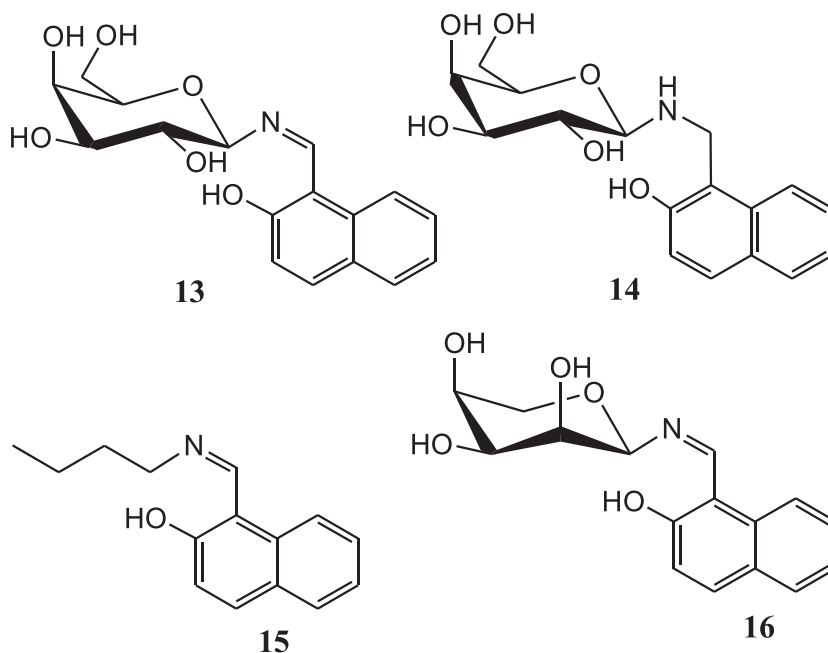

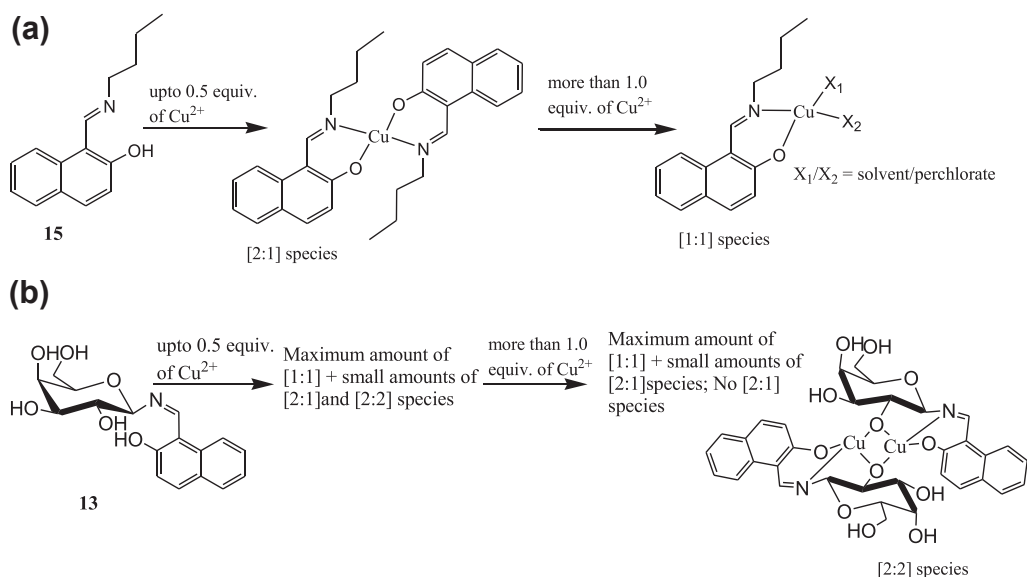**Fig. 10.** Structures of sugar-based sensor **13** and control compounds **14**–**16**.

Fig. 11. Existence of species based on the Q-TOF ES MS experiment: titration of (a) **15** and (b) **13** with Cu^{2+} ions.

3. Carbohydrate-based imino conjugate as sensors

The presence of imine functionality in metal sensors is highly in demand and acceptable owing to its effective role for cation sensing and easy synthesis [56–58]. The literature survey revealed that absorption and fluorescence studies of galactosyl-based naphthylimine derivative **13** (Fig. 10) exhibited selectivity toward Cu^{2+} ions in N-(2-hydroxyethyl)piperazine-N′-ethanesulfonic acid (HEPES) buffer at pH 7.2–7.4 [59]. The absorption and fluorescence spectral changes of **13** were observed in the presence of both ions Cu^{2+} and Zn^{2+} in MeOH system. Absorbance versus the $[M^{2+}/\mathbf{13}]$ mole ratio clearly suggested the formation of a 1:1 complex in case of Zn^{2+} and of a 1:2 complex for Cu^{2+} ions. The same binding ratios were obtained from fluorescence studies. However, the fluorescence studies of **13** in HEPES buffer at pH 7.2–7.4 exhibited altogether different results. The fluorescence intensity of **13** was gradually increased in the presence of Cu^{2+} only. The fluorescence was further quenched at higher and lower pH, namely, 6.0 and 5. To establish the function of imine and carbohydrate moiety of **13** for selective fluorogenic recognition of Cu^{2+}, Singhal et al. [59] have synthesized another three molecular systems **14**, **15**, and **16** (Fig. 10).
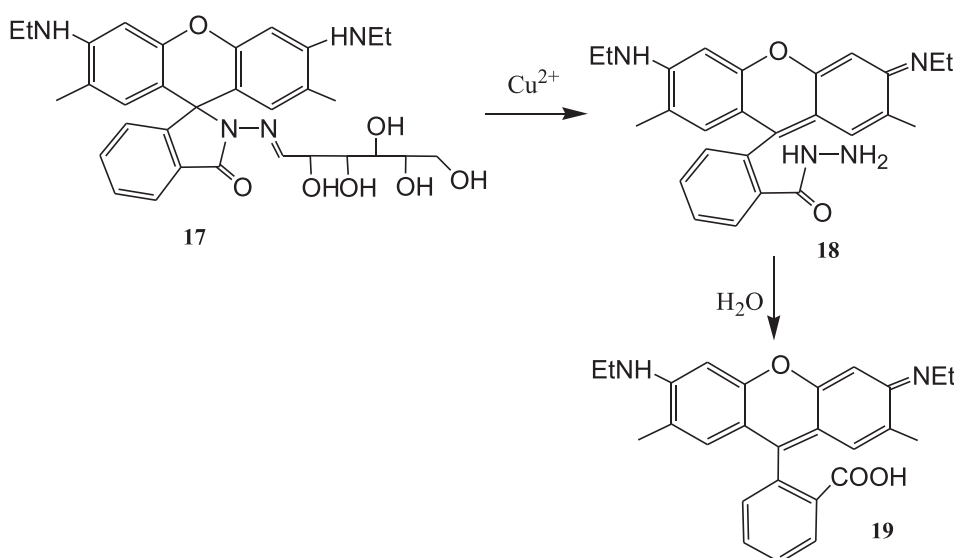

Fig. 12. Imine-linked sugar-rhodamine **17** and proposed reaction mechanism of **17** with Cu^{2+}.
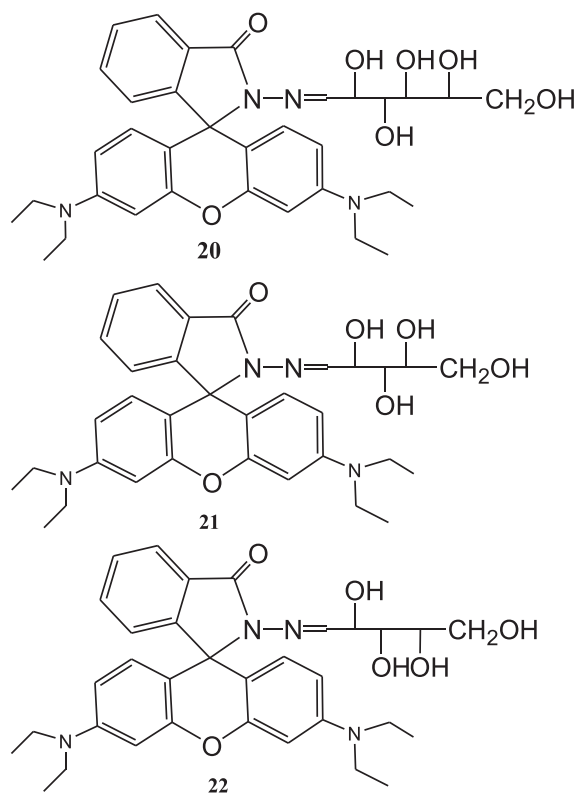
Fig. 13. Structure of carbohydrate-based sensors 20, 21, and 22.

(a)

(b)

Fig. 15. The structures of (a) sugar-rhodamine "turn-on" fluorescent sensor 25 and (b) reference compound 26.

Fluorescence titration of 14 with Cu^{2+} in buffer did not affect the fluorescence of 14, which clearly indicated that imine moiety of 13 is involved in the formation of the complex. Further titrations of 15 and 16 with Cu^{2+} resulted in an increase of fluorescence by 2.7 times and 2.3 times, respectively, which was attributed to the presence of imine and naphthylic −OH moieties in both compounds. The maximum increase of fluorescence intensity of 13 with Cu^{2+} as compared with 14, 15, and 16 revealed the C_2−OH

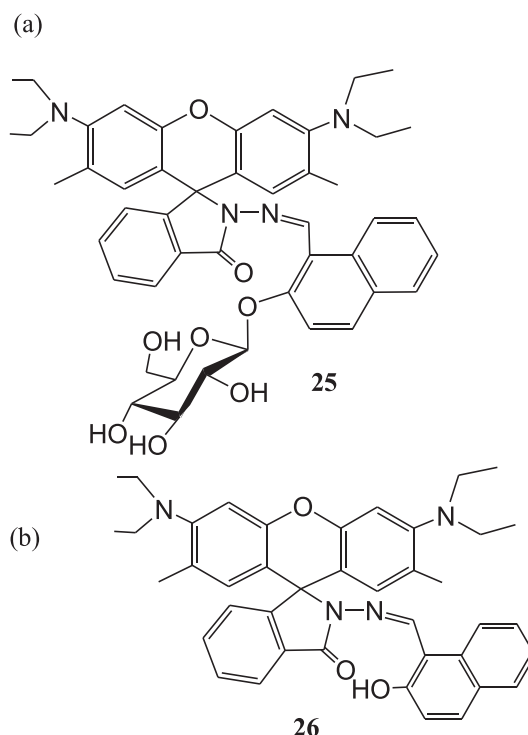of 13 to be also involved in the formation of the complex. The sensor 13 showed switch-on fluorescence property in the presence of Cu^{2+} ions. The 1:2 stoichiometry of the $13 \cdot Cu^{2+}$ complex was further established by Q-TOF ES MS titration of 13 and 15 with Cu^{2+} ions (Fig. 11). The quadrupole time-of-flight electrospray mass spectrometry (Q-TOF ES MS) titration of ligands with various concentrations of Cu^{2+} (0−0.2 equiv) suggested the existence of 1:1, 2:1, and 2:2 ligand metal species in the solution (Fig. 11). The binding constants of sensor 13 with Cu^{2+} were calculated as $50{,}500 \pm 1000$ M^{-1} and $50{,}500 \pm 700$ M^{-1} from
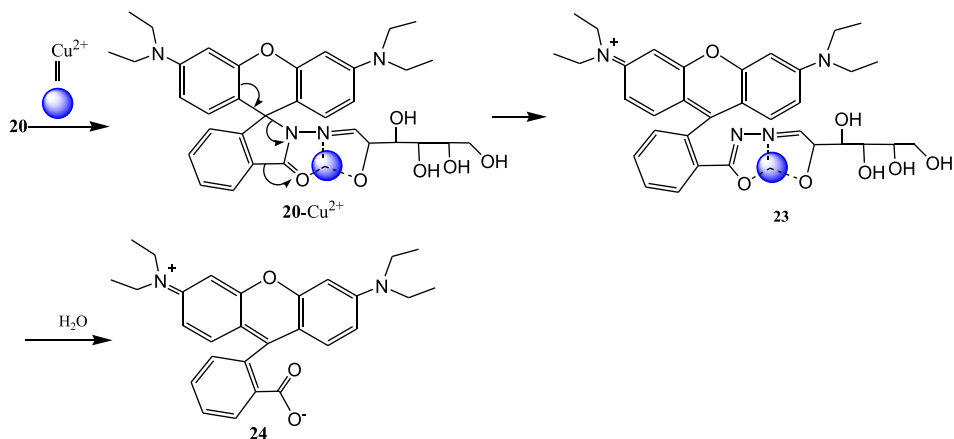

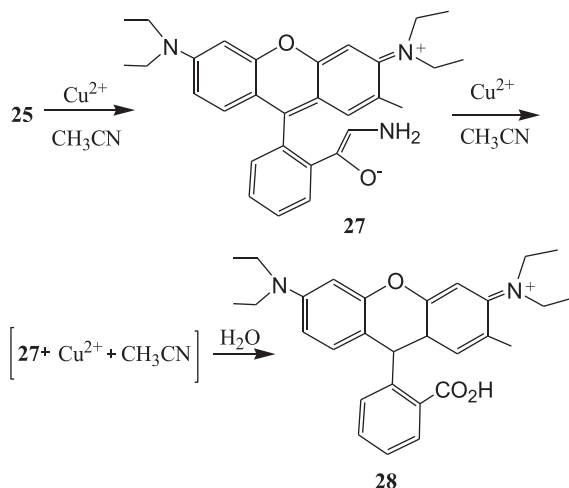Fig. 14. Proposed sensing mechanism of 20 with Cu^{2+}.

Fig. 16. Proposed reaction mechanism of sensor **25** with Cu^{2+}.

absorption and fluorescence titration experiments, respectively.

Ma et al. [60] developed a solvent-controlled fluorescence sensor **17** (Fig. 12) based on imine-linked sugar-rhodamine for selective detection of Cu^{2+} by the spirolactam ring–opening reaction in a 20% acetonitrile-water medium. The acetonitrile-water solution of sensor **17** is colorless and nonfluorescent. In the presence of Cu^{2+}, the aqueous solution (CH_3CN/H_2O, v/v, 1/4) of sensor **17** displayed a noticeable color change from colorless to pink along with enhancement of fluorescence intensity at room temperature. These phenomena were explained by the spirolactam ring opening and the formation of an acid derivative **19** (Fig. 12). The irreversible response of **17** to Cu^{2+} was established by EDTA experiments. The reaction mechanism (spirolactam ring opening) of sensor **17** with Cu^{2+} was confirmed by matrix-assisted laser desorption ionization (MALDI)-TOF mass spectroscopic analysis. The formation of compounds **18** and **19** after addition of Cu^{2+} in **17** was confirmed by HRMS spectrometry of the **17**·Cu^{2+} complex. Finally, the detection limit of sensor **17** toward Cu^{2+} was evaluated to be 12 μg/L (1.88×10^{-7} M). Interestingly, Huang et al. [61] observed that the synthesized sensor **17** showed high fluorometric selectivity toward Hg^{2+} in pure water system.

Zhang et al. [62] have reported three colorimetric and "off-on" fluorescent sensors **20**, **21**, and **22** based on rhodamine B and carbohydrates (Fig. 13). The selectivity of sensors toward Cu^{2+} ions was established by the measurements of absorbance and fluorescence of **20**, **21**, and **22** in CH_3CN-H_2O (2/3, v/v) solution before and after addition of 5 equiv of Cu^{2+} ions. All the three sensors exhibited remarkable fluorescence and absorbance enhancements in the presence of Cu^{2+} over other metal ions and anions. The 1:1 binding mode of both complexes was supported by ESI mass spectra and infrared measurements [63,64]. In the presence of Cu^{2+}, the spirolactam ring of sensors was opened and rhodamine B was formed, which was also established from ESI mass data. This phenomenon explained the significant enhancement of absorbance and fluorescence of sensors in the presence of Cu^{2+} ions. In addition, the detection limit for Cu^{2+} was calculated and found to be 1 ppm for all sensors. The proposed nonreversible binding mechanism of **20** through the formation of **23** and **24** is shown in Fig. 14 [65–67]. The sensors **21** and **22** exhibited similar binding mechanism with Cu^{2+} ions as illustrated in Fig. 14.

Yin et al. [68] reported another sugar-rhodamine "turn-on" fluorescent sensor **25** (Fig. 15) for selective detection of Cu^{2+} in acetonitrile. In the presence of Cu^{2+} ions, the fluorescence intensity of **25** was greatly enhanced in acetonitrile medium, whereas the fluorescence quenching was observed in water–acetonitrile medium. This phenomenon was explained by decreasing the oxidation ability of Cu^{2+} ions in water system. Strong fluorescence emission of **25** after addition of Cu^{2+} in CH_3CN was explained by spirolactam ring opening (Fig. 16). The irreversible nature of sensor **25** to Cu^{2+} was established by Cu^{2+} chelating agent, such as EDTA. The 1:2 stoichiometry of **25** with Cu^{2+} was calculated from Job plot experiments. However, the reference compound **26** (Fig. 15) exhibited 1:1 metal–ligand binding ratio, and response to Cu^{2+} was reversible. This result indicated that the sugar moiety in sensor **25** changed the reaction process. The reaction mechanism and the formation of intermediates **27**, **27** + Cu^{2+}+CH_3CN, and **28** (Fig. 16) were confirmed from MALDI-TOF mass spectral analysis of the **25**·Cu^{2+} complex. Finally, the limit of detection of Cu^{2+} with sensor **25** in acetonitrile was calculated to be 0.15 μM.

Mitra et al. [69] reported a diamino conjugate of glucosyl-cresol **29** (Fig. 17) for selective detection of Cu^{2+}
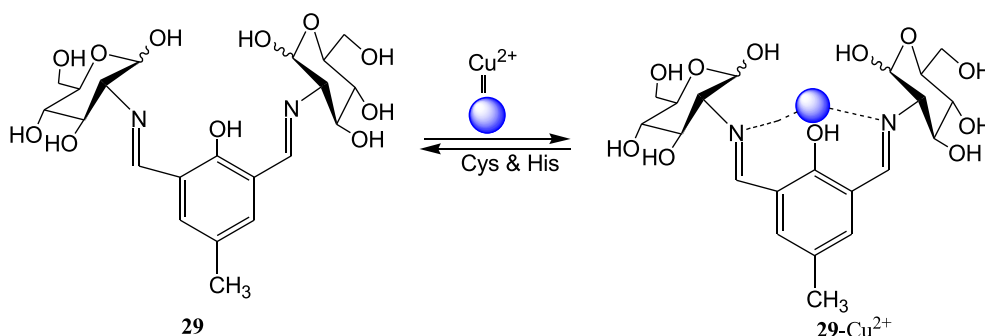

Fig. 17. Diamino conjugate of glucosyl-cresol **29** and proposed binding mode.
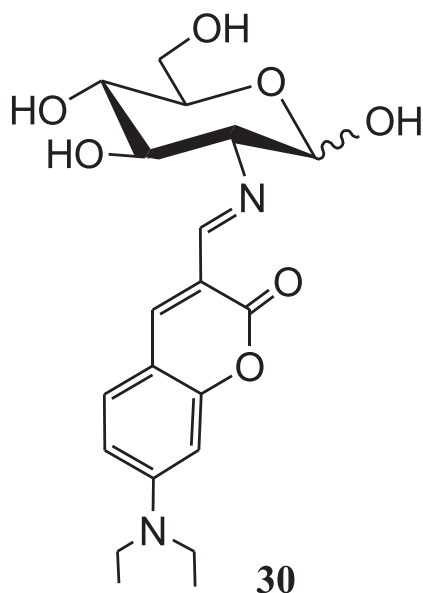
Fig. 18. Carbohydrate-based coumarin derivative **30**.

ions in ethanol. The selectivity of **29** toward Cu^{2+} ions was established by absorbance and fluorometric color studies. By the addition of Cu^{2+} to the ethanolic solution of **29**, the greenish fluorescent color of **29** turned to colorless. By the incremental addition of Cu^{2+} in the sensor solution, the absorption spectrum of **29** was shifted by 75 nm. In addition, the **29**·Cu^{2+} complex was used for recognition of cysteine and histidine (Fig. 17). Among the all naturally occurring amino acids, only cysteine and histidine bring back the original color of the sensor **29** after addition of the aforementioned amino acids in the **29**·Cu^{2+} complex solution. This result suggested that the displacement of Cu^{2+} from the **29**·Cu^{2+} complex occurred in the presence of amino acids (cysteine and histidine). In the original article [69], maybe they have drawn a D-sugar and an L-sugar on the same molecule.

The same group designed and synthesized another carbohydrate-based imino coumarin fluorescent sensor **30** (Fig. 18) for selective recognition of Cu^{2+} [70]. In the presence of Cu^{2+}, the fluorescent sensor **30** exhibited 95% fluorescence quenching and absorption change in aqueous HEPES buffer at pH 7–10, even in the presence of several cations. The formation of a complex between **30** and Cu^{2+} was established by the changes observed in fluorescence,
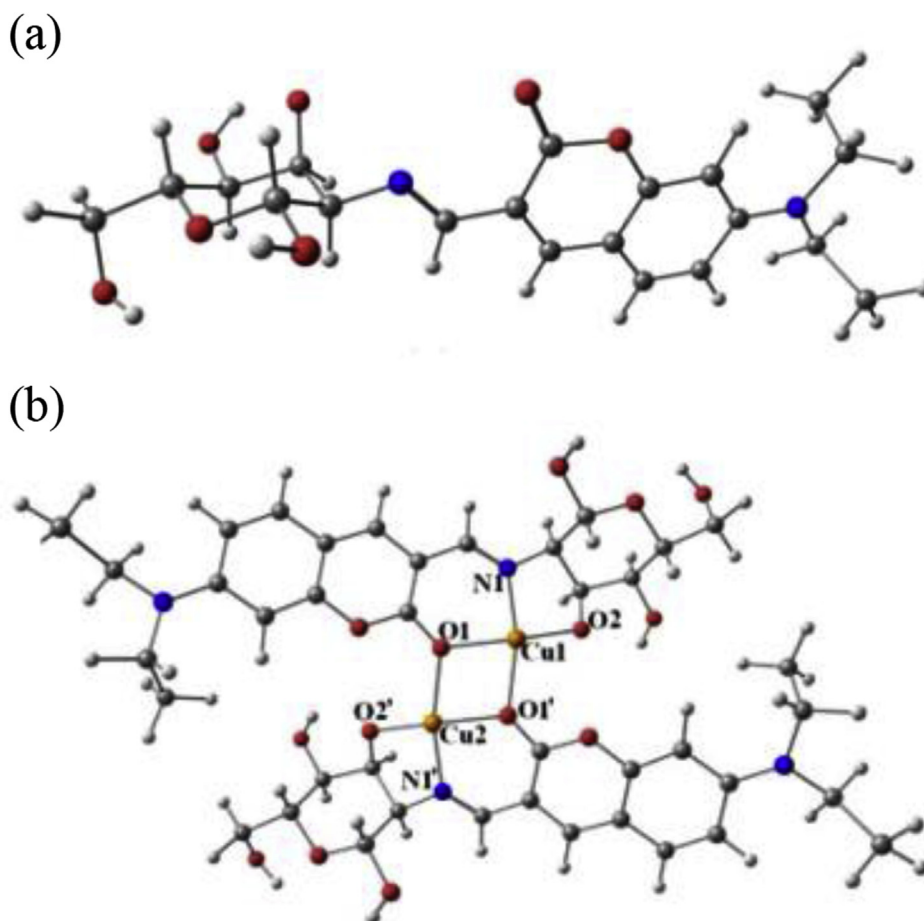

Fig. 19. DFT calculated optimized geometries of (a) **30** and (b) 2[**30**-Cu^{2+}] in methanol. DFT, density functional theory.
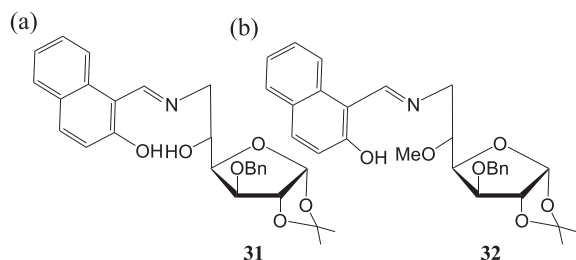
Fig. 20. Carbohydrate-based imine-linked (a) sensor **31** and (b) model compound **32**.

absorbance, ESI-MS, and ^{1}H NMR titrations. The Job plot suggested 1:1 stoichiometry of the complex, but actually, metal–ligand binding ratio of 2:2 was found from the ESI-MS spectrum of the copper complex. The DFT calculations were used to establish the structural modes of the [Cu**30**]$_2$ complex in both isomeric forms. DFT-optimized geometries of **30** and [Cu**30**]$_2$ are shown in Fig. 19. Silica gel sheet coated with sensor **30** was used to detect the Cu^{2+} through fluorometric color change. The developed silica gel strips coated with sensor **30** were used to detect Cu^{2+} up to a minimum concentration 5±1 μM. The sensor **30** can detect the copper ion up to a minimum concentration of 110±16 nM in HEPES buffer. Tridentate binding nature of **30** (both isomeric forms) with Cu^{2+} was established by ^{1}H NMR titration experiment and supported by DFT calculations. In

addition, sensor **30** showed effective fluorescence responses in the presence of Cu^{2+} in living cells.

A simple and easy-to-prepare imine-linked glucofuranose derivative **31** (Fig. 20a) has been reported by our group [71] for colorimetric detection of Cu^{2+} in semiaqueous medium. The carbohydrate-based sensor **31** exhibited a remarkable color change from yellow to colorless upon binding with Cu^{2+} in 20% acetonitrile–water. This selective color change was attributed to the remarkable absorption shift. More amusingly, the color and absorption of the **31**·Cu^{2+} complex could be restored by the addition of EDTA. The 1:1 stoichiometry of the **31**·Cu^{2+} complex was established by Job plot experiments [21] and further confirmed by the ESI-MS data of the complex. Furthermore, in terms of sensitivity, the limit of detection of the sensor **31** for Cu^{2+} was calculated to be 0.13 μM. To establish the binding mode of sensor **31**, the model compound **32** has been designed and synthesized (Fig. 20b). The binding mode of sensor **31** toward Cu^{2+} (Fig. 21a) was established on the basis of absorption measurement of synthesized model compound **32** with various cations, ^{1}H NMR titrations, and ESI-MS of the **31**·Cu^{2+} complex (Fig. 21a). The formation of complex **31a** is more favorable than that of **31b** because of tridentate ligand formation (imine and two hydroxyl groups). The binding mode of sensor **31** with Cu^{2+} proposed previously was further supported by DFT calculation, and it was concluded that triazole nitrogen and two hydroxyl groups are involved in the formation of the
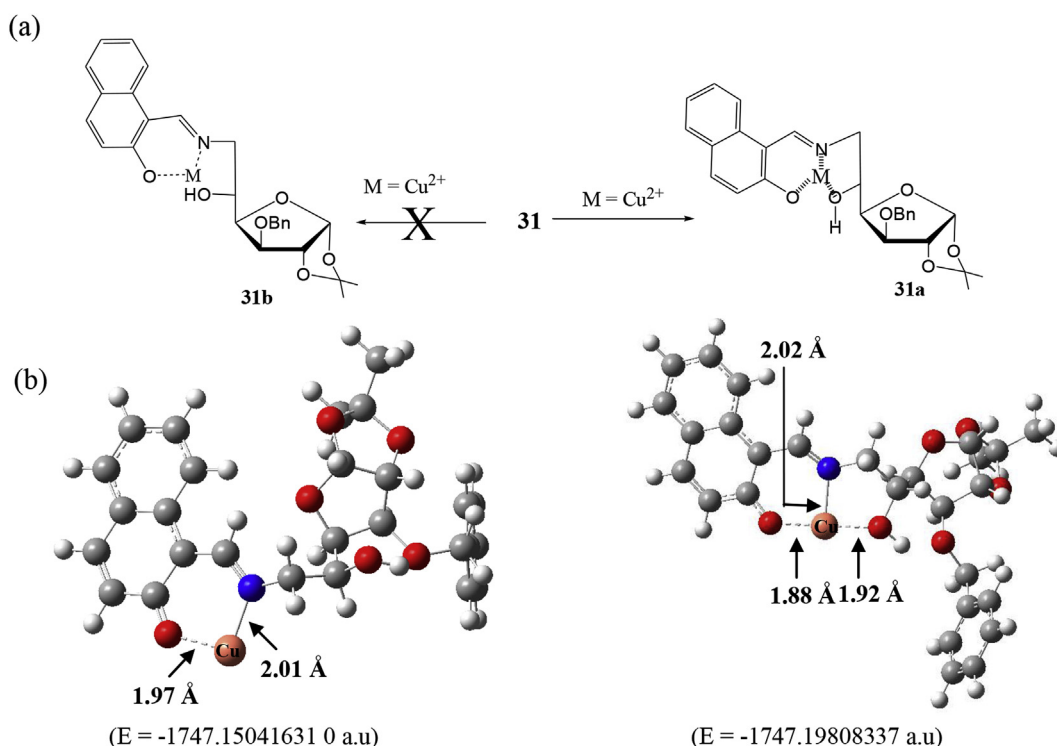

Fig. 21. (a) Proposed binding mode of sensor **31** with Cu^{2+}. (b) DFT-optimized structures of the proposed complexes. DFT, density functional theory.
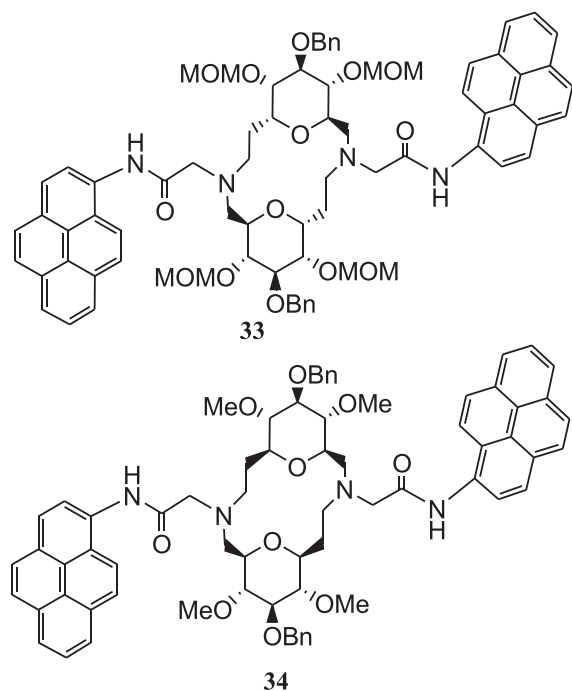
Fig. 22. Bispyrenyl sugar-aza-crown ethers **33** and **34**.

Fig. 24. Two pyrenylmethyl groups containing sugar-aza-crown (SAC) ether–based fluorescent sensor **35**.

31·Cu^{2+} complex after deprotonation of the aromatic −OH group (Fig. 21b).

4. Carbohydrate-based non–triazole-/imine-linked sensors

Two N-pyrenylacetamide–appended SAC ethers **33** and **34** (Fig. 22) have been designed and synthesized by Xie et al. [72] for selective recognition of Cu^{2+} ions in MeOH.

The complexation property of both the fluorescent molecular sensors with Cu^{2+} ions was established by absorption and fluorescence measurements. The fluorescence intensities of **33** and **3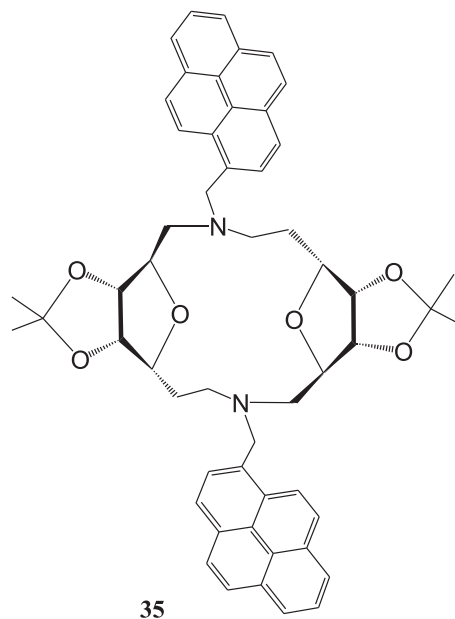4** were not affected by pH and other metal ions, such as Ca^{2+}, Mg^{2+}, Co^{2+}, Mn^{2+}, and Ni^{2+}. The

fluorescence intensity of both the sensors was remarkably induced in the presence of Cu^{2+} ions, which was explained by PET, from excited pyrene to the complexed Cu^{2+} cation [73]. The sensors showed to some extent fluorescence quenching effect with Pb^{2+}, Zn^{2+} (for **33**), and Cd^{2+} (for **34**). Both the sensors exhibited 1:1 metal–ligand binding ratio with high binding constants as log K (Cu^{2+}·**34**) = 6.7 ± 0.2 and log K (Cu^{2+}·**34**) = 7.8 ± 0.2. The detection limits of both the sensors were found to be 40 nM. The probable binding mode was established from DFT calculations, which suggested that two carbonyl groups and two N of SAC ethers take part in coordination (Fig. 23).

Hseih et al. [74] again reported another two pyrenylmethyl groups–containing SAC ether–based fluorescent sensor **35** (Fig. 24) for detection of Cu^{2+} and Hg^{2+} in MeOH. The fluorescence of **35** is measured in different
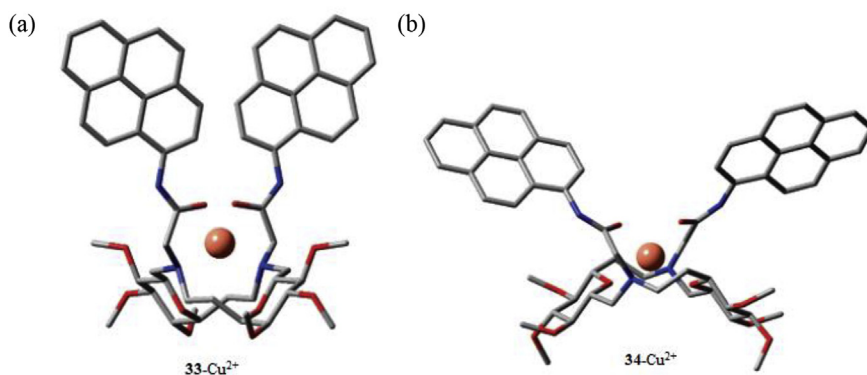

Fig. 23. DFT-calculated energy-minimized structures of the **33**·Cu^{2+} and **34**·Cu^{2+} complexes. (To simplify the DFT calculation, methyl ethers were considered as hydroxyl-protecting groups.) DFT, density functional theory.
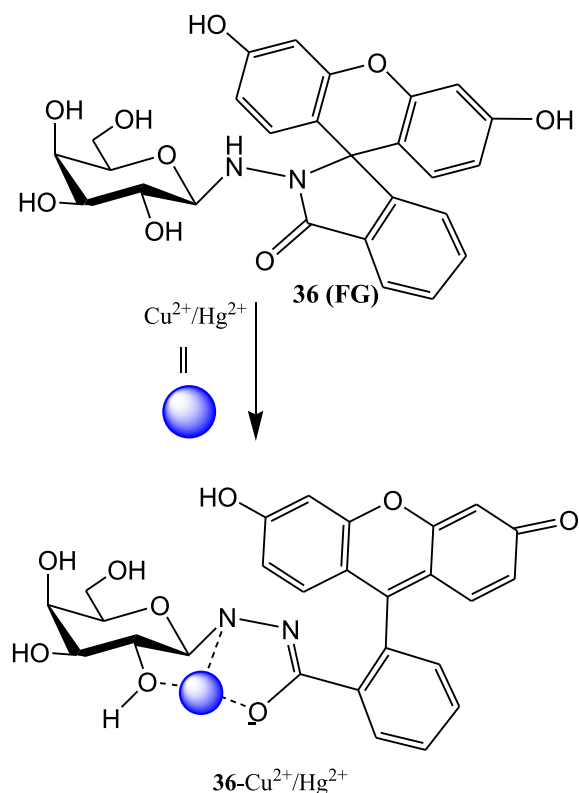
Fig. 25. Chemical structure of fluorescein-sugar conjugate **36** and proposed binding mode of **36** with Cu^{2+}/Hg^{2+}.

solvents (dichloromethane (DCM), MeOH, tetrahydrofuran (THF), CH_3CN, and dimethyl sulfoxide (DMSO)), and it was found that monomer and excimer ratio of **35** is not affected with the polarity of the solvents, whereas by increasing the polarity of solvents, only the monomer is predominant as compared with the excimer, in which the excimer emission is quenched completely because of strong solvation. This phenomenon indicated that two pyrenes of **35** do not exist parallel. In the presence of Cu^{2+} and Hg^{2+}, the fluorescence enhancement efficiency of sensor **35** was ~128% and 51% more than the free sensor. The fluorescence enhancement in the presence of Cu^{2+} and Hg^{2+} was explained by the PET process between the amino group of SAC ether and the pyrene fluorophore. The binding constant for the $35 \cdot Cu^{2+}$ complex was calculated as 7.4×10^1 M^{-1} from fluorescence titration data. The aforementioned fluorescence titration data were used to calculate the limit of detection of **35** for Cu^{2+} and found to be 1.3×10^{-4} M. The metal–ligand binding ratio of the $35 \cdot Cu^{2+}$ complex was established from the Job plot and supported by ESI-MS spectra of the complex. Hseih et al. [74] have established the binding mode of **35** toward Hg^{2+} ion by DFT calculation and concluded that two ribosyl ring oxygen atoms and two linker nitrogen atoms form coordination with Hg^{2+} in MeOH.

Diwan et al. [75] have reported nonfluorescent water-compatible fluorescein-sugar conjugate **36** (FG) for selective detection of Cu^{2+} ions (Fig. 25). The sensor **36** exhibited strong fluorescence and remarkable color change after spirolactam ring opening upon binding with Cu^{2+} ions in 70% aqueous HEPES buffer solution ($H_2O:CH_3CN = 70:30$, v/ v, pH 7.4). In the presence of Cu^{2+} ions, the absorbance of **36** was significantly increased in the visible region and concomitantly, color change was noticed from colorless to

Table 1
Characteristics of Cu^{2+}-selective reported sensors till date.

Sensor	Method	Solvent system	LOD	Binding constant	Ref
1	Fluorescence	MeOH	1.39 μM	4×10^5 M^{-1}	[37]
2	Fluorescence	MeOH	1.39 μM	2.5×10^4 M^{-1}	[41]
3	Fluorescence	MeOH	……	4.82×10^5 M^{-1}	[42]
4	Fluorescence	H_2O	0.89 μM	2.15×10^5 M^{-1}	[43]
6	UV-vis and fluorescence	CH_3CN	…..	$\log K = 5.64$	[44]
7	UV-vis	CH_3CN	0.75 μM	…….	[49]
8			……	…….	
9	Fluorescence	CH_3CN	6.99 μM	3.34×10^3 M^{-1}	[51]
10			7.30 μM	5.93×10^3 M^{-1}	
11	UV-vis	CH_3CN/phosphate buffer (1/4, v/v, pH 7.4)	3.50 μM	4.2×10^5 M^{-1}	[54]
13	UV-vis	HEPES buffer	…………	$50,500 \pm 1000$ M^{-1}	[59]
	Fluorescence			$50,500 \pm 700$ M^{-1}	
17	Fluorescence	CH_3CN/H_2O (1/4, v/v)	0.188 μM	……	[60]
20	UV-vis and Fluorescence	CH_3CN/H_2O (2/3, v/v)	15.7 μM	………	[62]
21					
22					
25	Fluorescence	CH_3CN	0.15 μM	…….	[68]
29	UV-vis and Fluorescence	EtOH	…..	…….	[69]
30	UV-vis and Fluorescence	Aqueous HEPES buffer with DMSO	0.11 ± 0.016 μM.	…….	[70]
31	UV-vis	CH_3CN/H_2O (1/4, v/v)	0.13 μM	9.7×10^5 M^{-1}	[71]
33	Fluorescence	MeOH	0.04 μM	$\log K = 6.7 \pm 0.2$	[72]
34				$\log K = 7.8 \pm 0.2$	
35	Fluorescence	MeOH	130 μM	7.4×10^1 M^{-1}	[74]
36	UV-vis	70% aqueous HEPES buffer ($H_2O:CH_3CN = 7:3$, v/v, pH = 7.4)	0.184 μM	$(1.02 \pm 0.08) \times 10^5$ M^{-1}	[75]
	Fluorescence		0.0063 μM	$(2.51 \pm 0.23) \times 10^6$ M^{-1}	

LOD: limit of detection [54].]

blue. These results suggested the spirolactam ring opening of FG in the presence of Cu^{2+}. The UV-vis spectrum of FG was also influenced in the presence of higher amount of Hg^{2+} ion. The fluorescence intensity of **36** was significantly increased in the presence of Cu^{2+}, but fluorescence was not affected by the addition of Hg^{2+} and other metal ions under the same experimental conditions. But the emission spectral pattern of FG was perturbed in the presence of Hg^{2+} at higher concentration of FG. In the presence of Cu^{2+} ions, the sensor showed strong blue-green fluorescence. The 1:1 metal—ligand (FG-Cu^{2+}) binding ratio was established from the Job plot and further confirmed by ESI-MS study of the **36**·Cu^{2+} complex. The association constants (K_a) for FG with Cu^{2+} were calculated from UV-vis and fluorescence titration data and found to be $(1.02 \pm 0.08) \times 10^5\ M^{-1}$ and $(2.51 \pm 0.23) \times 10^6\ M^{-1}$, respectively. The detection limits for Cu^{2+} were found to be $1.84 \times 10^{-7}\ M$ and $6.32 \times 10^{-9}\ M$ from absorbance and fluorescence spectroscopic methods, respectively [76,77]. Furthermore, the coordination mechanism was established from ^1H NMR titration experiment (Fig. 25).

Finally, the characteristics of reported Cu^{2+}-sensitive colorimetric and fluorometric carbohydrate-based sensors are demonstrated in Table 1.

5. Conclusion

In this minireview, we covered almost all the reported carbohydrate-based colorimetric and fluorometric sensors for recognition of Cu^{2+} ions. Our study revealed that limited numbers of carbohydrate-based Cu^{2+} sensors have been developed till date, although carbohydrate moiety has several advantages such as low cost, biocompatibility, presence of hydroxyl groups and oxygen atoms, and ring-flipping tendency. Some of the reported carbohydrate-based sensors act as potential sensors in terms of solubility, wavelength, nontoxicity, selectivity, and sensitivity. It is also noticed that some carbohydrate-based sensors for Cu^{2+} show poor water solubility because of inappropriate design. In this field, more research is required to design and develop effective sensors for detection of Cu^{2+} ions for real applications. The binding mechanism of sensors with Cu^{2+} ions was described successfully along with their DFT calculations which suggested that the solvent has a major role for specific selection of ions by the carbohydrate-based sensor. It is worth to mention that the structure of glucose in **17** and **23** reported in original articles [60,62] might be not correct. Finally, we can state that this review article will give the important way out for design and development of carbohydrate-based simple sensors for specific detection of metal ions in water medium and real-world applications.

Acknowledgements

References

[1i] J.A. Cowan, Inorganic Biochemistry: an Introduction, Wiley-VCH, New York, 1997, p. 133.
[2] M.C. Linder, M.H. Azam, Am. J. Clin. Nutr. 63 (1996) 797S—811S.
[3] E.L. Que, D.W. Domaille, C.J. Chang, Chem. Rev. 108 (2008) 1517—1549.
[4] Y.H. Chan, J. Chen, J.D. Batteas, Anal. Chem. 82 (2010) 3671—3678.
[5] J. Liang, M. Qin, R. Xu, X. Gao, Y. Shen, Q. Xu, Y. Cao, W. Wang, Chem. Commun. 48 (2012) 3890—3892.
[6] M. Shellaiah, Y.C. Rajan, H.C. Lin, J. Mater. Chem. 22 (2012) 8976—8987.
[7] T. Gupta, Provides a Detailed Description of Critical Next-Generation Materials and Technology for Microelectronics, Copper Interconnect Technology, 1st ed., Spinger, New York and London, 2009.
[8] N. Narayanaswamy, T. Govindaraju, Aldazine-based colorimetric sensors for Cu^{2+} and Fe^{3+}, Sens. Actuators B Chem. 161 (2012) 304—310.
[9] M.M.H. Khalil, A. Shahat, A. Radwan, M.F. El-Shahat, Sens. Actuators B Chem. 233 (2016) 272—280.
[10] P.C. Bull, G. Thomas, J.M. Rommens, J. Forbes, D. Cox, Nat. Genet. 5 (1993) 327—337.
[11] B. Sarkar, Chem. Rev. 99 (1999) 2535—2544.
[12] K.J. Barnham, C.L. Masters, A.I. Bush, Nat. Rev. Drug Discov. 3 (2004) 205—214.
[13] E. Gaggelli, H. Kozlowski, D. Valensin, G. Valensin, Chem. Rev. 106 (2006) 1995—2044.
[14] E. Madsen, J.D. Gitlin, Annu. Rev. Neurosci. 30 (2007) 317—337.
[15] B. High, D. Bruce, M.M. Richter, Anal. Chim. Acta 449 (2001) 17—22.
[16] X. Zhang, J. Fu, T.-G. Zhan, X.-Z. Wang, L. Dai, Y. Chen, X. Zhao, Tetrahedron Lett. 55 (2014) 6486—6489.
[17] WHO, Copper in Drinking Water: Background Document for Development of WHO Guidelines for Drinking-Water Quality, World Health Organization Geneva, 2004. WHO/SDE/WSH/03.04/88.
[18] A.P. de Silva, H.Q.N. Gunaratne, T. Gunnlaugsson, A.J.M. Huxley, C.P. McCoy, J.T. Rademacher, T.E. Rice, Chem. Rev. 97 (1997) 1515—1566.
[19] T. Gunnlaugsson, J.P. Leonard, N.S. Murray, Org. Lett. 6 (2004) 1557—1560.
[20] Y. Xiang, A.J. Tong, P.Y. Jin, Y. Ju, Org. Lett. 8 (2006) 2863—2866.
[21] H.M. Chawla, P. Munjal, P. Goel, J. Lumin. 164 (2015) 138—145.
[22] H.S. Jung, P.S. Kwon, J.W. Lee, J.I. Kim, C.S. Hong, J.W. Kim, S. Yan, J.Y. Lee, J.H. Lee, T. Joo, J.S. Kim, J. Am. Chem. Soc. 131 (2009) 2008—2012.
[23] L. Huang, X. Wang, G. Xie, P.X. Xi, Z.P. Li, M. Xu, Y.J. Wu, D.C. Bai, Z.Z. Zeng, Dalton Trans. 39 (2010) 7894—7896.
[24] P. Kaur, M. Kaur, K. Singh, Talanta 85 (2011) 1050—1055.
[25] S. Dalapati, S. Jana, M.A. Alam, N. Guchhait, Sens. Actuators B Chem. 160 (2011) 1106—1111.
[26] A. Kumar, V. Kumar, U. Diwan, K.K. Upadhyay, Sens. Actuators B Chem. 176 (2013) 420—427.
[27] H.M. Chawla, P. Goel, R. Shukla, Tetrahedron Lett. 55 (2014) 2173—2176.
[28] K. Ghosh, D. Tarafdar, A. Majumdar, C.G. Daniliuc, A. Samadder, A.R. Khuda-Bukhsh, Dipicolylamine coupled rhodamine dyes: new clefts for highly selective naked eye sensing of Cu^{2+} and CN^- ions, RSC Adv. 6 (2016) 47802—47812.
[29] N.K. Singhal, A. Mitra, G. Rajsekhar, M.M. Shaikh, S. Kumar, P. Guionneaub, C.P. Rao, Dalton Trans. (2009) 8432—8442.
[30] H. Yuasa, N. Miyagawa, T. Izumi, M. Nakatani, M. Izumi, H. Hashimoto, Org. Lett. 6 (2004) 1489—1492.
[31] H. Yuasa, N. Miyagawa, M. Nakatani, M. Izumi, H. Hashimoto, Org. Biomol. Chem. 2 (2004) 3548—3556.
[32] V.S.R. Rao, P.K. Qasba, P.V. Balaji, R. Chandrasekaran, Conformation of Carbohydarates, Harwood Academic Publishers, Amsterdam, 1998.
[33] H. Yuasa, H. Hashimoto, J. Am. Chem. Soc. 121 (1999) 5089—5090.
[34] R. Bielski, Z.J. Witczak, Chem. Rev. 113 (2013) 2205—2243.
[35] P. Thirumurugan, D. Matosiuk, K. Jozwiak, Chem. Rev. 113 (2013) 4905—4979.
[36] W. Xi, T.F. Scott, C.J. Kloxin, C.N. Bowman, Adv. Funct. Mater. 24 (2014) 2572—2590.
[37] Y.-C. Hsieh, J.-L. Chir, H.-H. Wu, P.-S. Chang, A.-T. Wu, Carbohydr. Res. 344 (2009) 2236—2239.
[38] A. Ojida, Y. Mito-oka, M.-A. Inoue, I. Hamachi, J. Am. Chem. Soc. 214 (2002) 6256—6258.
[39] A.P. de Silva, H.Q.N. Gunaratne, P.L.M. Lynch, J. Chem. Soc., Perkin Trans. 2 (1995) 685—690.
[40] M. Choi, M. Kim, K.D. Lee, K.-N. Han, I.-A. Yoon, H.-J. Chung, J. Yoon, Org. Lett. 3 (2001) 3455—3457.

[41] Y.-C. Hsieh, J.-L. Chir, H.-H. Wu, C.-Q. Guo, A.-T. Wu, Tetrahedron Lett. 51 (2010) 109–111.
[42] H.-J. Huang, H.-Y. Fang, J.-L. Chir, A.-T. Wu, Luminescence 26 (2011) 518–522.
[43] Y.-B. Chen, Y.-J. Wang, Y.-J. Lin, C.-H. Hu, S.-J. Chen, J.-L. Chir, A.-T. Wu, Carbohydr. Res. 345 (2010) 956–959.
[44] Y.-J. Zhang, X.-P. He, M. Hu, Z. Li, X.-X. Shi, G.-R. Chen, Dyes Pigments 88 (2011) 391–395.
[45] B. Valeur, I. Leray, Coord. Chem. Rev. 205 (2000) 3–40.
[46] L.Y. He, J.G. Cheng, T. Wang, C.M. Li, Z. Gong, H. Liu, et al., Chem. Phys. Lett. 462 (2008) 45–58.
[47] X.Z. You, The Structures and Properties of Coordination Compounds, Science Press, Beijing, 1992.
[48] S. Kaur, S. Kumar, Tetrahedron Lett. 45 (2004) 1–5.
[49] A. Thakur, S. Sardar, S. Ghosh, J. Chem. Sci. 124 (2012) 1255–1260.
[50] V. Lloveras, A. Caballero, A. Tárraga, M.D. Velasco, A. Espinosa, K. Wurst, D.J. Evans, J. Vidal-Gancedo, C. Rovira, P. Molina, J. Veciana, Eur. J. Inorg. Chem. (2005) 2436–2450.
[51] D. Kushwaha, R.S. Singh, V.K. Tiwari, Tetrahedron Lett. 55 (2014) 4532–4536.
[52] Y. Zhou, K. Liu, J.-Y. Li, Y. Fang, T.-C. Zhao, C. Yao, Org. Lett. 13 (2011) 1290–1293.
[53] Y.H. Lau, P.J. Rutledge, M. Watkinson, M.H. Todd, Chem. Soc. Rev. 40 (2011) 2848–2866.
[54] B. Dolai, S.I. Hazarika, S. Giri, A.K. Atta, Inorg. Chim. Acta 483 (2018) 496–503.
[55] Y.K. Jang, U.C. Nam, H.L. Kwon, I.H. Hwang, C. Kim, Dyes Pigments 99 (2013) 6–13.
[56] R. Joseph, J.P. Chinta, C.P. Rao, J. Org. Chem. 75 (2010) 3387–3395.
[57] B.M.J.M. Suijkerbuijk, B.N.H. Aerts, H.P. Dijkstra, M. Lutz, A.L. Spek, G. van Koten, R.J.M.K. Gebbink, Dalton Trans. (2007) 1273–1276.
[58] J.Y. Zhan, D.M. Tian, H.B. Li, New J. Chem. 33 (2009) 725–728.
[59] N.K. Singhal, B. Ramanujam, V. Mariappanadar, C.P. Rao, Org. Lett. 8 (2006) 3525–3528.
[60] X. Ma, Z. Tan, G. Wei, D. Wei, Y. Du, Analyst 137 (2012) 1436–1439.
[61] W. Huang, P. Zhou, W. Yan, C. He, L. Xiong, F. Li, C. Duan, J. Environ. Monit. 11 (2009) 330–335.
[62] D. Zhang, M. Wang, M. Chai, X. Chen, Y. Ye, Y. Zhao, Sens. Actuators B Chem. 168 (2012) 200–206.
[63] J.Y. Kwon, Y.J. Jang, Y.J. Lee, K.M. Kim, M.S. Seo, W. Nam, J. Yoon, J. Am. Chem. Soc. 127 (2005) 10107–10111.
[64] X. Zeng, L. Dong, C. Wu, L. Mu, S.-F. Xue, Z. Tao, Sens. Actuators B Chem. 141 (2009) 506–510.
[65] X. Chen, T. Pradhan, F. Wang, J.S. Kim, J. Yoon, Chem. Rev. 112 (2012) 1910–1956.
[66] Z. Xu, L. Zhang, R. Guo, T. Xiang, C. Wu, Z. Zheng, F. Yang, Sens. Actuators B Chem. 156 (2011) 546–552.
[67] Z.-C. Wen, R. Yang, H. He, Y.-B. Jiang, Chem. Commun. (2006) 106–108.
[68] J. Yin, X. Ma, G. Wei, D. Wei, Y. Du, Sens. Actuators B Chem. 177 (2013) 213–217.
[69] A. Mitra, S. Areti, A.K. Mittal, S. Bhakta, C.P. Rao, Trends In Carbohydr. Res. 5 (2013) 20–24.
[70] S. Areti, J.K. Khedkar, S. Bandaru, R. Teotia, J. Bellare, C.P. Rao, Anal. Chim. Acta 873 (2015) 80–87.
[71] B. Dolai, A. Bhaumik, N. Pramanik, K.S. Ghosh, A.K. Atta, J. Mol. Struct. 1164 (2018) 370–377.
[72] J. Xie, M. Menand, S. Maisonneuve, R. Metivier, J. Org. Chem. 72 (2007) 5980–5985.
[73] K. Rurack, Spectrochim. Acta, Part A 57 (2001) 2161–2195.
[74] Y.-C. Hsieh, J.-L. Chir, S.-T. Yang, S.-J. Chen, C.-H. Hu, A.-T. Wu, Carbohydr. Res. 346 (2011) 978–981.
[75] U. Diwan, A. Kumar, V. Kumar, K.K. Upadhyay, P.K. Roychowdhury, Sens. Actuators B Chem. 196 (2014) 345–351.
[76] IUPAC, Spectrochim. Acta B 33 (1978) 241–245.
[77] USEPA (209), Fed. Regist. 49 (October) (1984) 43430 (also referred to as "40 CFR Part 136").